

Ground state energy density, susceptibility, and Wilson ratio of a two-dimensional disordered quantum spin system

J.-H. Peng,¹ D.-R. Tan,¹ and F.-J. Jiang^{1,*}

¹*Department of Physics, National Taiwan Normal University, 88, Sec.4, Ting-Chou Rd., Taipei 116, Taiwan*

A two-dimensional (2D) spin-1/2 antiferromagnetic Heisenberg model with a specific kind of quenched disorder is investigated, using the first principles nonperturbative quantum Monte Carlo calculations (QMC). The employed disorder distribution has a tunable parameter p which can be considered as a measure of the corresponding randomness. In particular, when $p = 0$, the disordered system becomes the clean one. Through a large scale QMC, the dynamic critical exponents z , the ground state energy densities E_0 , as well as the Wilson ratios W of various p are determined with high precision. Interestingly, we find that the p dependence of z and W are likely to be complementary to each other. For instance, while the z of $0.4 \leq p \leq 0.9$ match well among themselves and are statistically different from $z = 1$ which corresponds to the clean system, the W for $p < 0.7$ are in reasonable good agreement with that of $p = 0$. The technical subtlety of calculating these physical quantities for a disordered system is demonstrated as well. The results presented here are not only interesting from a theoretical perspective, but also can serve as benchmarks for future related studies.

PACS numbers:

I. INTRODUCTION

Spatial dimension two is extraordinary from a theoretical point of view. This is because according to the famous Mermin-Wagner theorem, for finite systems with short-range interactions, continuous symmetries cannot be broken spontaneously at any temperature $T > 0$ [1–6]. As a result, for two-dimensional (2D) quantum spin antiferromagnets (AF), the associated studies have been focusing on certain exotic finite temperature properties of the systems. Particularly, several universal quantities are predicted and verified numerically. Such a temperature region where these unusual universal features exist is called the quantum critical regime (QCR) in the literature and has been explored in detail during the last few decades. [7–19].

For 2D quantum spin AF system, whenever QCR is mentioned, it typically refers to a finite temperature region. However, such an exotic regime extends to zero temperature at a quantum critical point (QCP). In addition, the (finite T) region above a QCP is where these profound characteristics can be uncovered the most clearly [14, 19].

A physical observable, namely the spinwave velocity c plays an important role in those mentioned universal quantities of QCR for the 2D spin-1/2 antiferromagnets. For instance, the value of c without doubt has great impact on the determinations of two universal quantities of QCR, namely $\chi_u c^2/T \sim 0.27185$ and $c/(T\xi) \sim 1.04$. Here χ_u and ξ are the uniform susceptibility and the correlation length, respectively [10, 14, 19]. In the phase with long-range antiferromagnetic order, c can be calculated efficiently using the spatial and the temporal wind-

ing numbers squared [18, 20, 21].

Considering a clean 2D spin-1/2 AF which comes with a given spatial arrangement of two types of antiferromagnetic couplings J' and J ($J' > J$), by tuning the ratio J'/J (i.e. the system is dimerized) a QCP may appear when J'/J exceeds a certain value $(J'/J)_c$. The dynamic critical exponent z associated with such a kind of QCP takes the value of 1. For a QCP g_c which is obtained by varying the associated parameter g , the physical quantity c scales as $c \propto (g - g_c)^{\nu(z-1)}$ close to g_c [10, 13], where ν is the correlation length exponent. As a result, c is a constant when the related z of a QCP is 1. For 2D quantum AF systems, the QCPs induced by dimerization introduce above belong exactly to this case. When disorder is present, $z > 1$ and c is zero at g_c . Consequently, certain universal quantities of QCR cannot be calculated in a direct manner for disordered systems.

While for a 2D disordered quantum spin antiferromagnet, certain quantities of QCR such as $\chi_u c^2/T$ cannot be directly accessed, yet some observables do not encounter the difficulty that c cannot be calculated with ease. One of them, namely the Wilson ratio W [10, 17, 18], which will be defined later, is one of the main topics of our study presented here. In particular, we investigate the behavior of W with respect to the strength of randomness, which is controlled by a parameter $p \geq 0$, of the employed disorder distribution. Here $p = 0$ corresponds to the clean case. Apart from W , the dynamic critical exponents z as well as the ground state energy densities E_0 of several values of p considered in this study are determined as well.

To carry out the proposed investigation, we have performed a large scale quantum Monte Carlo calculation (QMC). In addition, several p are considered and the simulations are done at the corresponding critical point $g_c(p)$ of each studied p . Based on our numerical results, we find the magnitude of E_0 grows monotonically with

*fjjiang@ntnu.edu.tw

$g_c(p)$ (hence p as well since $g_c(p) \propto p$ as shown in [22]), similar to that of the correlation length exponent ν [22]. Interestingly, the p dependence of z and W are likely to be complementary to each other. For instance, while the z of $0.4 \leq p \leq 0.9$ match well among themselves and are statistically different from $z = 1$ which corresponds to the clean system, the W for $p < 0.7$ are in reasonable good agreement with that of $p = 0$ ($W \sim 0.1243$). The subtlety of calculating these physical quantities for a disordered system is demonstrated here as well. Our investigation is important and interesting in itself from a theoretical perspective. In particular, the obtained outcomes can be used as benchmarks for future related studies.

The rest of this paper is organized as follows. After the introduction, the studied model, the employed disorder distribution as well as the relevant observables are described. Following that we present our results. In particular, the numerical evidence for the mentioned complementary relation for z and W are demonstrated. Finally, a section concludes our study.

II. MICROSCOPIC MODELS AND OBSERVABLES

The model investigated in our study has been described in detail in Refs. [22, 23]. Here we briefly summarize certain technical perspectives of the considered system. The Hamiltonian of the investigated 2D disordered spin-1/2 herringbone Heisenberg model (on the square lattice) is given by

$$H = \sum_{\langle ij \rangle} J \vec{S}_i \cdot \vec{S}_j + \sum_{\langle i'j' \rangle} J' \vec{S}_{i'} \cdot \vec{S}_{j'}, \quad (1)$$

where in Eq. (1) J (which are set to 1 here) and J' are the antiferromagnetic couplings (bonds) connecting nearest neighboring spins $\langle ij \rangle$ and $\langle i'j' \rangle$, respectively, and \vec{S}_i is the spin-1/2 operator at site i . In this study we use the convention $J' > J$. Fig. 1 is a cartoon representation of the considered model. The quenched disorder introduced into the system is based on the one employed in Refs. [22, 23]. Specifically, for every bold bond in fig. 1, its antiferromagnetic strength J' takes the value of $1+(g-1)(1+p)$ or $1+(g-1)(1-p)$ with equal probability. Here $g > 1$ and $0 \leq p \leq 1$. With the used conventions, the average and difference for these two types of bold bonds J' are given by g and $2p(g-1)$, respectively. In addition, p can be thought of as a measure for the disorder of the studied model as well.

To perform the proposed calculations of determining the ground state energy density E_0 , the dynamic critical exponent z , and the Wilson ratio W for the considered disordered system (with various p), the uniform susceptibility χ_u , the internal energy density E , and the specific heat C_V (as functions of the temperature T or the inverse temperature β) are measured in our simulations.

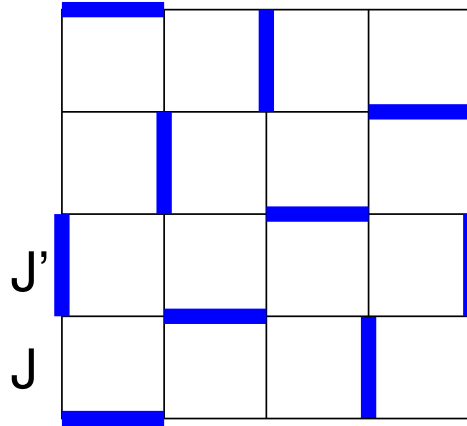


FIG. 1: The 2D dimerized spin-1/2 herringbone Heisenberg model on the square lattice investigated in this study. The antiferromagnetic coupling strengths for the thick and thin bonds are J' and J , respectively.

The uniform susceptibility χ_u is defined by

$$\chi_u = \frac{\beta}{L^2} \left\langle \left(\sum_i S_i^z \right)^2 \right\rangle, \quad (2)$$

where β and L are the inverse temperature and linear box size used in the simulations, respectively. Furthermore, the internal energy density E and the specific heat C_V are given as

$$E = \frac{1}{L^2} \langle H \rangle, \quad (3)$$

$$C_V = \frac{\partial E}{\partial T}. \quad (4)$$

Using these observables, E_0 , z , and W for various p of the studied disordered model can be determined with high precision.

III. THE NUMERICAL RESULTS

For each of the considered values of $p = 0.0, 0.2, 0.4, 0.5, 0.6, 0.7, 0.8$, and 0.9 , to calculate the associated desired physical quantities, we have carried out large-scale QMC using the stochastic series expansion (SSE) algorithm with very efficient operator-loop update [24, 25]. The simulations are done at the corresponding critical points $g_c(p)$ for these chosen p . In addition, for every p , several hundred to few thousand randomness configurations with $L = 128$ and (or) $L = 256$ are generated. Each configuration is produced with its own random seed and then is used for all the calculations of the considered values of β .

A. The strategy of calculating the Wilson ratio W

In the framework of SSE, the quantities of internal energy density E and specific heat C_V can be obtained

by

$$E = -\frac{1}{L^2} \left(\langle n \rangle / \beta - \frac{1}{4} \sum_b J_b \right), \quad (5)$$

$$C_V = \frac{1}{L^2} (\langle n^2 \rangle - \langle n \rangle^2 - \langle n \rangle), \quad (6)$$

respectively, where the summation is over all the bonds b and n is the number of nonidentity operators in the SSE operators sequence (operators string).

Based on the large- N expansion of the relevant effective field theory, at the associated critical point it is predicted that for clean systems the (leading) low- T behavior of χ_u , E , and C_V are given by

$$\chi_u \sim \frac{1.0760}{\pi c^2} T, \quad (7)$$

$$E \sim E_0 + \frac{2.8849}{\pi c^2} T^3, \quad (8)$$

$$C_V \sim \frac{8.6548}{\pi c^2} T^2, \quad (9)$$

respectively, where the c appearing above is the spinwave velocity. With these leading T -dependence of χ_u , E and C_V , the Wilson ratio W can be expressed as

$$W = \frac{\chi_u T}{C_V} \sim 0.1243. \quad (10)$$

While C_V can be calculated directly from its definition $C_V = \partial E / \partial T$ (or $C_V = \frac{1}{L^2} (\langle n^2 \rangle - \langle n \rangle^2 - \langle n \rangle)$), as being shown in the literature, such a approach will lead to very noisy results at the region of low temperature [18]. In addition, the fact that c is zero at the QCP of a disordered system prevents one from determining c directly. Motivated by the method outlined in Ref. [18], here we calculate W through the following procedures.

Firstly, from the β -dependence of the internal energy density E , namely

$$E(\beta) = E_0 + a\beta^{-1-2/z} \quad (11)$$

(here z is the dynamic critical exponent), one obtains a and z . Then the specific heat C_V , as a function of β , can be written as

$$C_V = a(1 + 2/z)\beta^{-2/z}. \quad (12)$$

Secondly, the β -dependence of χ_u is fitted to the expression

$$\chi_u(\beta) = b\beta^{1-2/z}. \quad (13)$$

Finally, using Eqs. 12 and 13, one arrives at the following formula for W

$$W = \frac{b}{a(1 + 2/z)}. \quad (14)$$

In other words, instead of using C_V directly, here W is calculated through the coefficients z , a and b obtained from fitting the data of χ_u and E to their expected T -dependence ansatzes Eqs. 11 and 13.

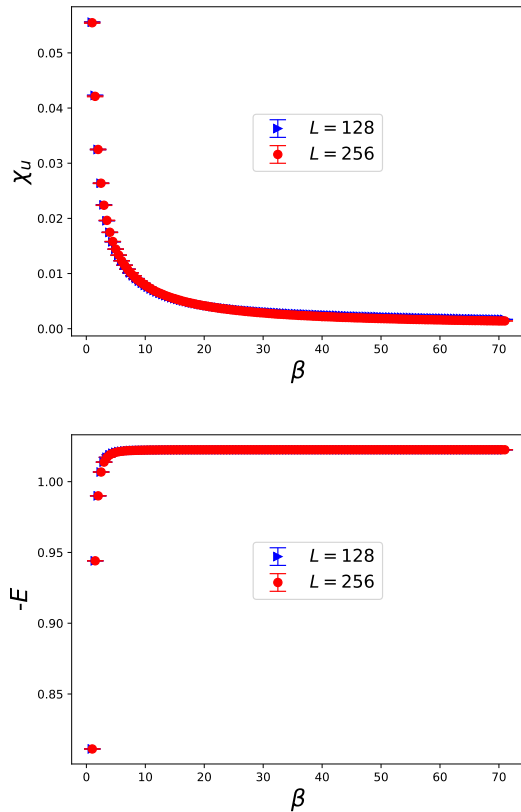


FIG. 2: χ_u (top) and minus (internal) energy density E (bottom) as functions of β for $p = 0.0$. The shown errors are the corresponding mean errors.

B. The obtained χ_u and E from simulations

The obtained data of χ_u and $-E$ for $p = 0.0, 0.4, 0.6$, and 0.9 are depicted in figs. 2, 3, 4 and 5. Both data of $L = 128$ and $L = 256$ are put in these figures in order to demonstrate that the outcomes of $L = 256$ are (most likely) sufficient for size convergence.

C. The analysis results associated with the clean model

For the clean model $p = 0$, it is well known that $z = 1$. Hence, z will be fixed to 1 in our analysis for $p = 0$. As a result, the following ansatz

$$\chi_u = a_0 + aT + a_1 T^2 \quad (15)$$

is considered to fit the χ_u data of $p = 0$. Apart from that, the formula used to fit the data of E for $p = 0$ is Eq. 11 with $z = 1$ as well.

By investigating the relevant data for $L = 128$ and $L = 256$, the finite size effect begins to appear when $\beta > 16.0$. Therefore the data of $L = 256$ with $\beta \leq 24.0$ are used for the fits. We have additionally carried out fits using the $L = 256$ data of $\beta \leq 20.0$ and have found that these new results lead to a value of W which agrees

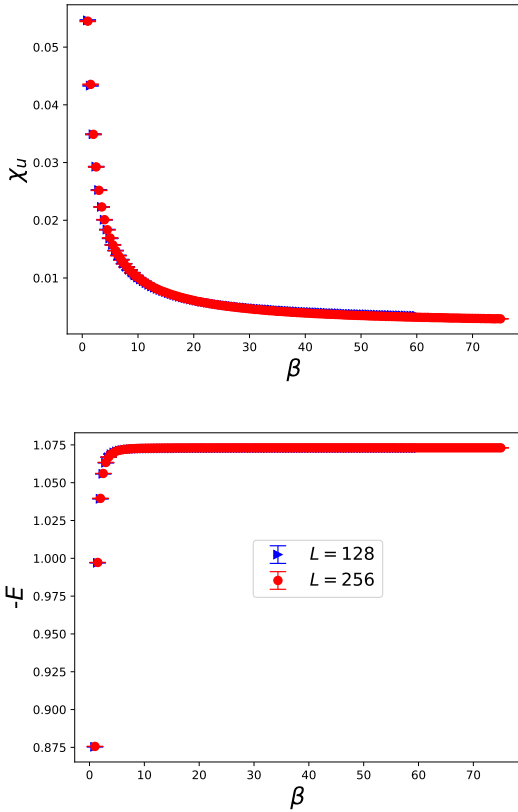


FIG. 3: χ_u (top) and minus (internal) energy density E (bottom) as functions of β for $p = 0.4$. The shown errors are the corresponding mean errors.

quantitatively with that obtained using the $L = 256$ data of $\beta \leq 24.0$. For each of data with a fixed range of β , in addition to taking care of finite size effect, the following procedures are adopted to calculate the corresponding W .

Firstly, a bootstrap resampling (with respect to β) is conducted simultaneously for both χ_u and E . Secondly, fits for these obtained resampled data are performed. Finally W is determined using the outcomes of these fits. In these mentioned fits, Gaussian noises are considered as well. The above described steps are carried out for twenty thousand times and only those outcomes with both χ^2/DOF (DOF stands for degrees of freedom) of the two fits (for χ_u and E) being smaller than 3.0 are included as the candidate results of W . The resulting W , as well as its associated uncertainty, quoted for this set of data with that given fixed range of β are the mean and the standard deviation of these candidate results.

We have conducted several calculations using various range of β , and each of these calculations comes with its own results (mean and uncertainty) for W . Moreover, to estimate the means and errors of the desired quantities appropriately, the weighted bootstrap resampling method is applied to all the mentioned results of W . Specifically, for every randomly generated data set (W_j, σ_{W_j}) obtained using the bootstrap procedure (σ_{W_j} is the standard deviation associated with W_j), the result-

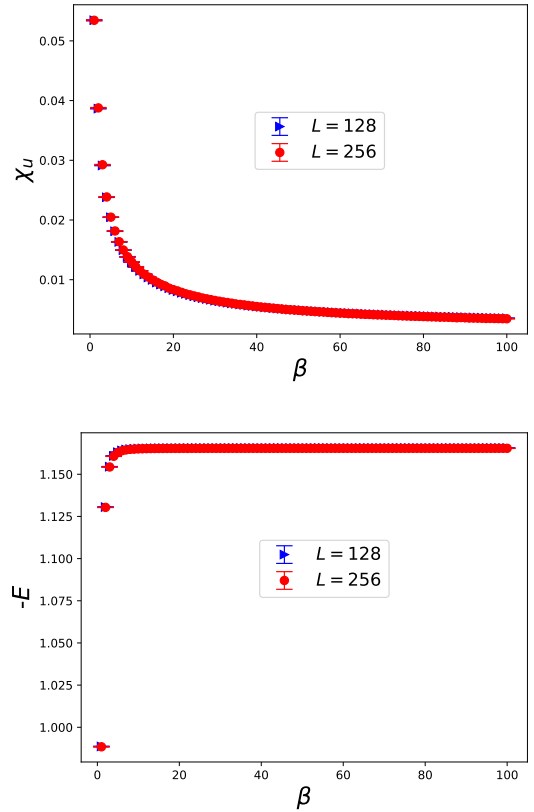


FIG. 4: χ_u (top) and minus (internal) energy density E (bottom) as functions of β for $p = 0.6$. The shown errors are the corresponding mean errors.

ing mean is given by

$$\frac{\sum_i \frac{1}{\sigma_{W_i}^2} W_i}{\sum_i \frac{1}{\sigma_{W_i}^2}}. \quad (16)$$

The reason for the use of above equation (called weighted mean in this study) is as follows. Notice that data with large standard deviations are less accurately determined than those with small standard deviations. As a result, those large standard deviation data should contribute less weight to the determination of the associated mean.

After carrying out twenty thousand weighted bootstrap resampling steps, the resulting W is estimated to be $W = 0.1238(3)$. The obtained $W = 0.1238(3)$ agrees very well with the theoretical prediction $W = 0.1243$. This confirms the validity of the procedures introduced above for the calculation of W .

The ground state energy density for the clean model is calculated by the same procedure and is given by $E_0 = -1.022523(1)$.

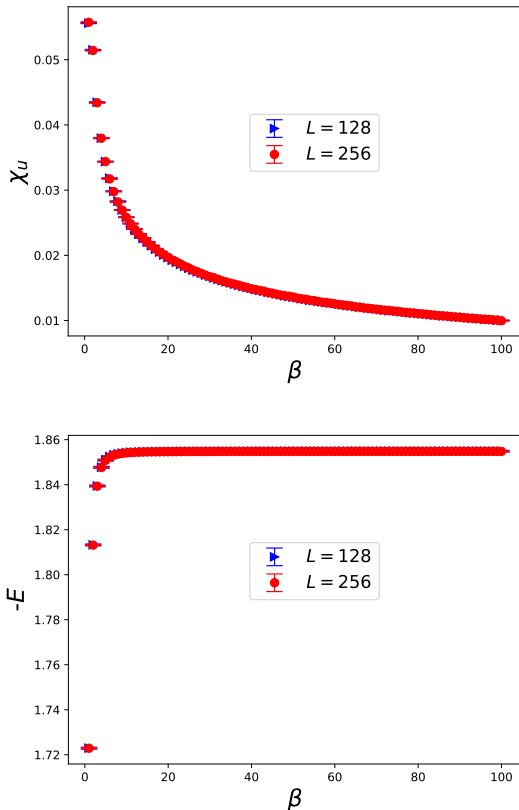


FIG. 5: χ_u (top) and minus (internal) energy density E (bottom) as functions of β for $p = 0.9$. The shown errors are the corresponding mean errors.

D. The results of the disordered model with various randomness strength p

Since each generated configuration is used for all the simulations of the considered β , for a given set of $p > 0$ and L , the data themselves are correlated. Hence, to accurately estimate the associated errors for the coefficients in the fitting ansatzes, one should employ the correlated least χ^2 method for the analysis. However, the stability of the correlated least χ^2 method varies and depends on the quality of the data used for the fits. Moreover, biased outcomes may be reached if the associated covariance matrix for a given data set contains eigenvalues which have very small magnitude. Using the rule of thumb that the ansatz considered to fit correlated data should contain as few (to be determined) parameters as possible, we adopt the following approach to calculate E_0 , z , and W for $p > 0$.

First of all, for each β the bootstrap resampling method is performed for the raw data resulting from the generated disordered configurations. Second of all, these resampled data are used to calculate the disordered average of χ_u and E which are then considered for the relevant fits. Here the data employed for the fits of χ_u and E have different range of β . Indeed, as can be seen from figs. 3, 4, 5, for all the considered $p > 0$ the associated E reaches its ground state value E_0 quickly, while this is

not the case for χ_u . As a result, it is more appropriate to use different range of β for the fits of χ_u and E .

After carrying out the fit of χ_u , the obtained result of z is employed as an input for the fit of E . When both fits of χ_u and E are done, the resulting results are then put back to calculate the associated correlated χ^2/DOF . Here a cut-off for the eigenvalues of the associated covariance matrix is imposed in order to avoid biased results. These introduced steps are performed for many times, and only those results which have correlated χ^2/DOF smaller than 3.0 for both the fits of χ_u and E are considered for later calculations. Finally for each of the considered p , the above procedures have been applied to many sets consisting of various range of β . Each of these sets (The whole sets is denoted by S) has its own results (mean and standard deviation) of E_0 , z , and W as well as the number of successful calculations.

For a considered p , the final quoted results of E_0 , z , and W in this study are estimated by a bootstrap resampling procedure using the following formula to calculate the mean of every resampled data from S .

$$\frac{\sum_i N_i O_i / \sigma_{O_i}^2}{\sum_i N_i / \sigma_{O_i}^2}, \quad (17)$$

where $\{O_i\}$, $\{\sigma_{O_i}\}$ and $\{N_i\}$ stand for the randomly picked outcomes in S , the associated standard deviations, as well as the related numbers of (successful calculated) results of these picked outcomes, respectively. Finally, such a resampling step is conducted for several thousand times, and the numerical values presented here for these considered physical quantities are the resulting means and standard deviations (estimated conservatively) of this procedure. The uncertainties of E_0 calculated by the described steps are much smaller than those of the original E_0 contained in S . Hence, for the data in S we have also calculated their associated weighted errors. The dominant one of these two estimations, namely the standard deviations and the weighted errors, are the final values quoted here.

The E_0 , z and W as functions of p calculated by the procedures introduced above are shown in figs. 6, 7, 8. The related results for the clean model are shown in these figures as well for comparison.

The E_0 as a function of p shows a monotonic behavior in magnitude, which is similar to that of the correlation length exponents ν obtained in Ref. [22].

Regarding the z presented in the figure, one observes that the magnitude of z increases with p until p reaches a specific $p_c < 0.4$. For $p \geq 0.4$, all the calculated values of z lie between (around) 1.3 and (around) 1.4. If one takes into account the systematic errors due to the uncertainties of $g_c(p)$, then the z for $p \geq 0.4$ are fairly close to each other. The solid and dashed lines in fig. 7 represent the mean and standard deviation for all the values of z associated with $p \geq 0.4$ (including both those of $L = 128$ and $L = 256$). These guided lines justify the claim made above. This phenomenon is consistent

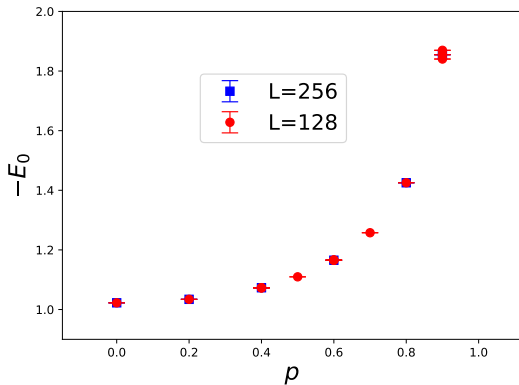


FIG. 6: $-E_0$ as functions of p . The results are obtained from the analysis using the correlated χ^2 described in the main text. The solid squares and solid circles are for $L = 256$ and $L = 128$, respectively. For some values of p , the $L = 128$ results contains those corresponding to g_c , the lower and upper bounds of g_c .

with the one shown in Ref. [31], where the calculated z corresponding to various parameters take a universal value. We would like to point out that when conducting the determination of z from χ_u , the obtained results are somehow a little bit sensitive to the considered fitting range of χ_u . This motivates the use of the resampling procedures described above. In conclusion, our analysis indicates that it is subtle to calculate the quantity z and a careful strategy is needed.

Finally, in fig. 8 we demonstrate the results of W as functions of p obtained from the analysis outlined previously. Intriguingly, similar to the scenario of z , for those W corresponding to $p < 0.7$, their values are more or less close to each other. The solid and dashed lines in the figure again stand for the mean and standard deviation for all the W with their associated p satisfy $p < 0.7$ (including both those of $L = 128$ and $L = 256$). Considering the impact resulting from the errors of $g_c(p)$, the scenario that W take the same value (or at least values close to each other) for all the p such that $p < 0.7$ is probable. Interestingly, the correlation length exponent ν is beginning to fulfill the Harris criterion when $p > 0.8$ and this is where the magnitude of W increases sharply. This observation implies that there may exist a relation between W and fulfillment of Harris criterion.

IV. DISCUSSIONS AND CONCLUSIONS

In this study, we calculate the Wilson ratio W of a 2D spin-1/2 antiferromagnetic Heisenberg model with a specific quenched disorder, using the first principle non-perturbative quantum Monte Carlo simulations. The employed disorder distribution has a tunable parameter p which can be considered as a measure of randomness. The W of the clean case as well as that of $p = 0.2, 0.4, 0.5, 0.6, 0.7, 0.8, 0.9$ are determined with high precision. The critical dynamic exponents z and the

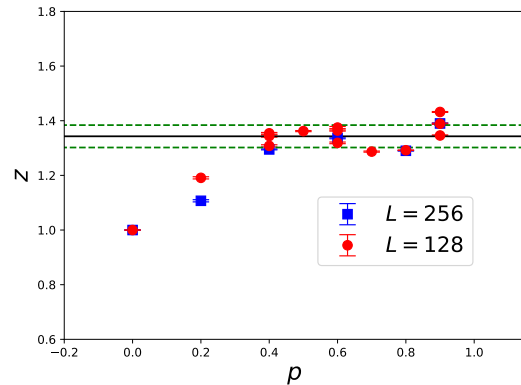


FIG. 7: z as functions of p . The results are obtained from the analysis using the correlated χ^2 described in the main text. The solid squares and solid circles are for $L = 256$ and $L = 128$, respectively. For some values of p , the $L = 128$ results contains those corresponding to g_c , the lower and upper bounds of g_c . The solid and dashed lines in the figure represent the mean and standard deviation for all the z such that their associated p satisfy $p \geq 0.4$ (including both those of $L = 128$ and $L = 256$).

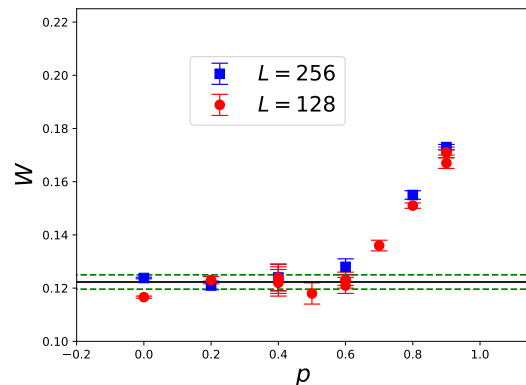


FIG. 8: W as functions of p . The results are obtained from the analysis using the correlated χ^2 described in the main text. The solid squares and solid circles are for $L = 256$ and $L = 128$, respectively. For some values of p , the $L = 128$ results contains those corresponding to g_c , the lower and upper bounds of g_c . The solid and dashed lines in the figure represent the mean and standard deviation for all the W such that their corresponding p satisfy $p < 0.7$ (including both those of $L = 128$ and $L = 256$).

ground state energy densities E_0 are obtained as well.

Remarkably, for the considered system with the employed quenched disorder, the p dependence of W and z seems to be complementary to each other. The obtained z are likely to take a universal value for $p \geq 0.4$. This agrees with the outcomes determined in Ref. [31]. In addition, the calculated W for $0 < p < 0.7$ also have a trend of stay close to the result $W \sim 0.1243$ of the clean model ($p = 0$). In particular, the value of W begins to increase sharply when p is approaching $p = 0.9$ where the Harris criterion is fulfilled. Considering the fact that with what conditions the Harris criterion is valid is still not known [26–37], the results presented here may shed

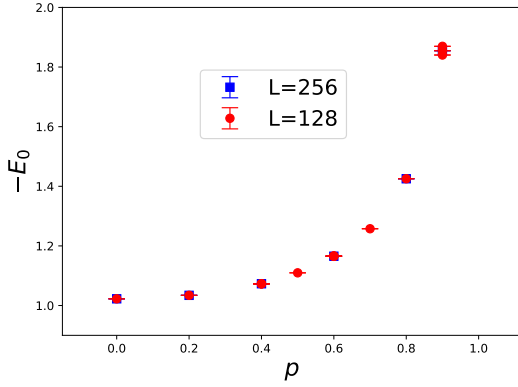


FIG. 9: $-E_0$ as functions of p . The results are obtained from the analysis using the conventional uncorrelated χ^2 . The solid squares and solid circles are for $L = 256$ and $L = 128$, respectively. For some values of p , the $L = 128$ results contains those corresponding to g_c , the lower and upper bounds of g_c .

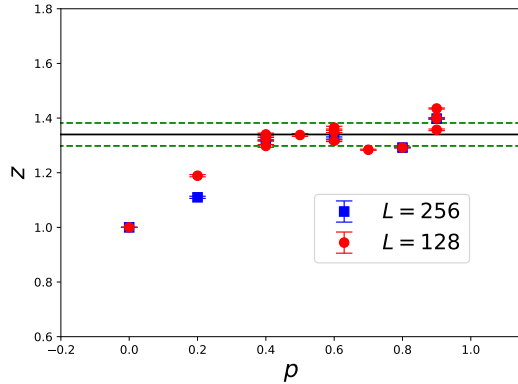


FIG. 10: z as functions of p . The results are obtained from the analysis using the conventional uncorrelated χ^2 . The solid squares and solid circles are for $L = 256$ and $L = 128$, respectively. For some values of p , the $L = 128$ results contains those corresponding to g_c , the lower and upper bounds of g_c . The solid and dashed lines in the figure represent the mean and standard deviation for all the z such that their associated p satisfy $p \geq 0.4$ (including both those of $L = 128$ and $L = 256$).

some light on setting up some useful guidelines to decide whether the Harris criterion is valid for a given disorder distribution.

Apart from the subtlety of calculating z described previously, the determination of W is extremely non-trivial as well. Indeed, the W estimated here is based on Eq. 14 which contains two constants a and b . Since a is a sub-leading coefficient in the associated ansatz, it is sensitive to the range of β used for the fits as well. Careful strategy and resampling procedure are conducted in this study in order to calculate W accurately.

If the correlations among the data of various values of β are ignored, then the same resampling steps as well as the criterion of $\chi^2/\text{DOF} < 3$ (here the χ^2 is the conventional uncorrelated χ^2 , not the correlated χ^2 described in the main text) introduced in previous sections will lead to figs. 9, 10, and 11. Remarkably, while the outcomes

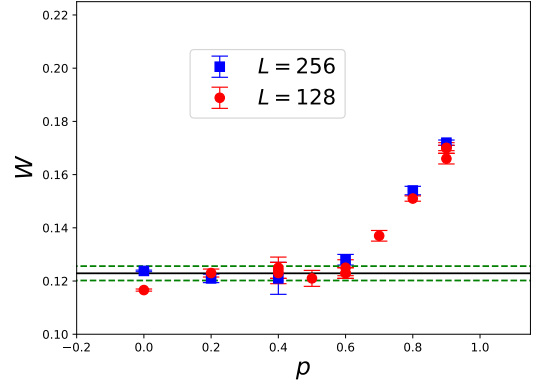


FIG. 11: W as functions of p . The results are obtained from the analysis using the conventional uncorrelated χ^2 . The solid squares and solid circles are for $L = 256$ and $L = 128$, respectively. For some values of p , the $L = 128$ results contains those corresponding to g_c , the lower and upper bounds of g_c . The solid and dashed lines in the figure represent the mean and standard deviation for all the W such that their corresponding p satisfy $p < 0.7$ (including both those of $L = 128$ and $L = 256$).

of z shown in fig. 10 are slightly different from those in fig. 7, the E_0 and W presented in figs. 9 and 11 agree very well with the ones demonstrated in figs. 6 and 8. In particular, the trend claimed from the analysis associated with the correlated χ^2 regarding the p dependence of z and W , namely being complementary to each other, is valid as well for the outcomes obtained using the conventional uncorrelated χ^2 (i.e. figs. 10 and 11). This observation seems to reconfirm the conclusions resulting from investigating some lattice quantum chromodynamics data outlined in Refs. [38, 39].

To summarize, the outcomes resulting from the investigations carried out here, specially the obtained numerical results of E_0 , z , and W , are not only important accomplishments, but also can be considered as benchmarks for future related studies.

This study is partially supported by MOST of Taiwan.

[1] N. D. Mermin and H. Wagner, Phys. Rev. Lett. **17**, 1133 (1966).

[2] P. C. Hohenberg, Phys. Rev. **158**, 383 (1967).

[3] Sidney Coleman, Communications in Mathematical

- Physics volume 31, pages 259264 (1973).
- [4] Axel Gelfert and Wolfgang Nolting, *J. Phys.: Condens. Matter* **13** R505 (2001).
 - [5] J. Cardy, *Scaling and Renormalization in Statistical Physics*, Cambridge University Press, Cambridge, UK, 1996.
 - [6] S. Sachdev, *Quantum Phase Transitions* (Cambridge University Press, Cambridge, 2nd edition, 2011).
 - [7] S. Chakravarty, B. I. Halperin, and D. R. Nelson, *Phys. Rev. B* **39**, 2344 (1989).
 - [8] A. V. Chubukov and S. Sachdev, *Phys. Rev. Lett.* **71**, 169 (1993).
 - [9] A. V. Chubukov and S. Sachdev, *Phys. Rev. Lett.* **71**, 2680 (1993).
 - [10] A. V. Chubukov, S. Sachdev, and J. Ye, *Phys. Rev. B* **49**, 11919 (1994).
 - [11] A. W. Sandvik, A. V. Chubukov, and S. Sachdev, *Phys. Rev. B* **51**, 16483 (1995).
 - [12] M. Troyer, H. Kantani, and K. Ueda, *Phys. Rev. Lett.* **76**, 3822 (1996).
 - [13] Matthias Troyer, Masatoshi Imada, and Kazuo Ueda, *J. Phys. Soc. Jpn.* **66**, 2957 (1997).
 - [14] Jae-Kwon Kim and Matthias Troyer, *Phys. Rev. Lett.* **80**, 2705 (1998).
 - [15] Y. J. Kim, R. J. Birgeneau, M. A. Kastner, Y. S. Lee, Y. Endoh, G. Shirane, and K. Yamada, *Phys. Rev. B* **60**, 3294 (1999).
 - [16] Y. J. Kim and R. J. Birgeneau, *Phys. Rev. B* **62**, 6378 (2000).
 - [17] A. W. Sandvik, V. N. Kotov, and O. P. Sushkov, *Phys. Rev. Lett.* **106**, 207203 (2011).
 - [18] A. Sen, H. Suwa, and A. W. Sandvik, *Phys. Rev. B* **92**, 195145 (2015).
 - [19] D.-R. Tan and F.-J. Jiang, *Phys. Rev. B* **98**, 245111 (2018).
 - [20] F.-J. Jiang, *Phys. Rev. B* **83**, 024419 (2011).
 - [21] F.-J. Jiang and U.-J. Wiese, *Phys. Rev. B* **83**, 155120 (2011).
 - [22] Jhao-Hong Peng, L.-W. Huang, D.-R. Tan, and F.-J. Jiang, *Phys. Rev. B* **101**, 174404 (2020).
 - [23] Nvsen Ma, Anders W. Sandvik, and Dao-Xin Yao, *Phys. Rev. B* **90**, 104425 (2014).
 - [24] A. W. Sandvik, *Phys. Rev. B* **66**, R14157 (1999).
 - [25] A. W. Sandvik, *AIP Conf. Proc.* **1297**, 135 (AIP, New York, 2010).
 - [26] A. B. Harris, *J. Phys. C* **7**, 1671 (1974).
 - [27] J. T. Chayes, L. Chayes, D. S. Fisher, and T. Spencer, *Phys. Rev. Lett.* **57**, 2999 (1986).
 - [28] O. Motrunich, S.C. Mau, D.A. Huse, and D.S. Fisher, *Phys. Rev. B* **61**, 1160 (2000).
 - [29] A. W. Sandvik, *Phys. Rev. Lett.* **89**, 177201 (2002).
 - [30] O. P. Vajk and M. Greven, *Phys. Rev. Lett.* **89**, 177202 (2002).
 - [31] R. Sknepnek, T. Vojta, and M. Vojta, *Phys. Rev. Lett.* **93**, 097201 (2004).
 - [32] Rong Yu, Tommaso Roscilde, and Stephan Haas, *Phys. Rev. Lett.* **94**, 197204 (2005).
 - [33] A. W. Sandvik, *Phys. Rev. Lett.* **96**, 207201 (2006).
 - [34] T. Vojta, *J. Low Temp. Phys.* **161**, 299 (2010).
 - [35] Dao-Xin Yao, Jonas Gustafsson, E. W. Carlson, and Anders W. Sandvik, *Physical Review B*, **82**, 172409 (2010).
 - [36] Thomas Vojta, *AIP Conference Proceedings* **1550**, 188 (2013).
 - [37] Thomas Vojta and José A. Hoyos, *Phys. Rev. Lett.* **112**, 075702 (2014).
 - [38] C. Michael, *Phys. Rev. D* **49**, 2616 (1994).
 - [39] C. Michael and A. McKerrill, *Phys. Rev. D* **51**, 3745 (1995).